

## THE SMALL SCALE STRUCTURE OF N103B - NATURE OR NURTURE?

KAREN T. LEWIS, DAVID N. BURROWS, GORDON P. GARMIRE,  
JOHN A. NOUSEK

*THE STATE UNIVERSITY OF PENNSYLVANIA, 525 DAVEY  
LABORATORY, UNIVERSITY PARK, PA, 16802, USA*

JOHN P. HUGHES

*DEPARTMENT OF PHYSICS AND ASTRONOMY, RUTGERS  
UNIVERSITY, 126 FRELINGHUYSEN ROAD, PISCATAWAY, NJ  
08854, USA*

PATRICK SLANE

*HARVARD-SMITHSONIAN CENTER FOR ASTROPHYSICS, 60  
GARDEN STREET, MA, 02138, USA*

**Abstract.** We present new results from a 40.8 ks *Chandra* ACIS observation of the young supernova remnant (SNR) N103B located in the Large Magellanic Cloud. The high resolution *Chandra* image reveals structure at the sub-arcsecond level, including several bright knots and filaments. Narrow-band imaging and spatially resolved spectroscopy reveal dramatic spectral variations in this remnant as well. In this paper we discuss whether these variations are due to inhomogeneities in the surrounding environment or were generated in the explosion which created the SNR.

### 1. Introduction

N103B, one of the brightest X-ray and radio sources in the Large Magellanic Cloud (LMC), is a young, compact ( $D=7\text{pc}$  or  $30''$ ) supernova remnant (SNR). The remnant lies on the north-eastern rim of the H II region N103 and is only 40 pc from the young star cluster NGC 1850 (Dickel & Milne 1995). At radio and X-ray wavelengths, N103B has a shell-like morphology with the western half being  $\sim 3$  times brighter than the eastern half (Fig 1). The  $H\alpha$  image is dominated by 4 bright knots in the west, but also shows a partial shell as well (Williams et al. 1999). Due to its proximity to a star forming region, it was originally suspected that N103B was the result of the core collapse of a massive object. However, the ASCA spectrum shows no evidence for K-shell emission from O, Ne or Mg while Si, S, Ar, Ca, and Fe features are strong, indicating that the remnant is more likely the result of a Type Ia SN explosion (Hughes et al. 1995).

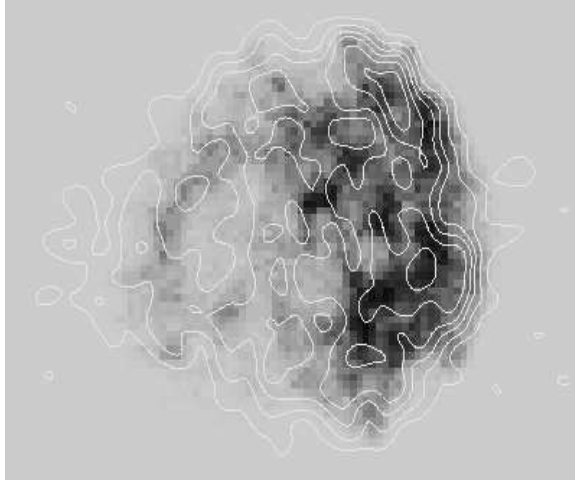


Figure 1. Plot of X-ray image with 2.5 cm ATCA contours (Dickel & Milne 1995). Contours are 1.7, 1.3, 0.9, 0.6, 0.3, and 0.1 mJy/beam. The spatial resolution of the radio data is  $1.2''$ , which is slightly larger than that of *Chandra*.

## 2. Observations & Reduction

N103B was observed for 40.8 ks on 4 December 1999 using the back-illuminated *Chandra* ACIS-S3 detector. The data were corrected for Charge Transfer Inefficiency (CTI) as described in Townsley et al. (2001a). The data were then cleaned and filtered with the standard CIAO 2.1 software packaged. The ASCA grade filter (g02346) was used throughout. The background was selected from an annulus ( $r_{in} = 60''$ ,  $r_{out} = 120''$ ). We employ the response matrices created by Townsley et al. (2001b) to match the CTI-corrected data.

## 3. Analysis & Results

### 3.1. Brightness Variations

The most striking structural feature in N103B is the large brightness contrast between the eastern and western halves of the remnant, which is present in the radio, X-ray, and, to some extent,  $H\alpha$  images. A cloud of absorbing material *could* produce the observed brightness variation in X-ray. However, this same cloud would not absorb the radio synchrotron emission. The radio and X-ray brightness are generally very well correlated (Scronce et al., this proceedings), thus it is much more likely that this brightness variation is due to a density contrast between the eastern and western halves of the remnant.

In the high-resolution *Chandra* image, the western half of the remnant has been resolved into several filaments and bright knots, which roughly co-incide with the  $H\alpha$  knots. (The optical image is not yet publicly available for direct comparison.) The spectra of these knots do not show an enhancement of the heavy elements, so it is unlikely that they are “bullets” of ejecta. One possibility is that the  $H\alpha$  knots, which show the normal LMC abundances, (Russel & Dopita

1992) are actually dense clumps in the H II region. As the dense cloudlets are heated by the shock, some of the material will be evaporated and heated to X-ray emitting temperatures, leading to an enhancement of the X-ray emission around the dense H $\alpha$  clumps. Thus, many of the large brightness variations, on both large and small spatial scales, are likely to be caused by inhomogeneities in the surrounding environment.

### 3.2. Narrow Band Imaging

We have extracted images of the remnant in the He-like Si, H-like Si, and S lines. The continuum was estimated by performing a linear interpolation between two regions on either side of the line. The Continuum Subtracted (CS) and Equivalent Width (EW) images for He-like Si are shown in Fig. 2 ab. The CS image is quite similar to the 0.5-8 keV image (Fig. 1). The EW image, however, reveals a striking ring-like structure near the rim of the remnant. To ensure that the ring-like structure is statistically significant, the image was collapsed into the radial and azimuthal dimensions (Fig. 2cd). As can be seen, the EW of He-like Si increases radially with little azimuthal dependence. A similar structure is seen in the H-like Si and S EW images. The spectra of the innermost and outermost rings are shown in Fig. 3; the increase in equivalent width of Si and S, as well as Ar, is clear.

### 3.3. Spectral Analysis

The increase in EW could be the result of temperature, ionization or abundance variations. To determine the true cause, we divided the remnant into seven annuli, each with  $\sim 35,000$  counts, and performed detailed spectral modeling on each.

We use a non-equilibrium ionization (NEI) model developed by Jack Hughes along with two absorbing columns: one for the galaxy and another for absorption within the LMC. The NEI model allows for each element to have independent temperatures and ionization states, which can be linked as desired. To reproduce the spectra we find it necessary to have three thermodynamic “phases”, each of which contributes both to the line and continuum emission. The predominant source of emission arises from a highly ionized ( $n_e t \geq 10^{12.5}$  s/cm<sup>3</sup>), 0.9 keV plasma containing H, Si, S, and Ar. To reconcile the emission from the L-shell transitions of Fe and Ca with the strong K $\alpha$  line of these elements, it is necessary to place Fe and Ca (as well as H) in a very high temperature ( $\geq 3$ keV), low ionization ( $n_e t \sim 10^{10-11}$  s/cm<sup>3</sup>) plasma. It is reasonable for Fe to be in a high temperature, low ionization state since radioactive decay of Ni into Fe will locally heat the Fe clumps, forming hot, diffuse “bubbles” of Fe. A similar effect has been seen in Tycho’s Remnant, another type Ia SNR (Hwang et al. 1998). Finally, the O, Ne, and Mg emission is not consistent with the high ionization state of the Si, S, and Ar. Thus we have a third plasma which contains H, O, Ne, and Mg with an ionization timescale of  $n_e t \sim 10^{11}$  s/cm<sup>3</sup>. The temperature is not well constrained, but is consistent with 0.9 keV. Finally, a Gaussian component at 0.72 keV was required in all but the outermost rings. We believe that there may be several Fe L-shell transitions that are missing in the model.

An example fit is shown in Fig. 4. We find that, within error bars, the

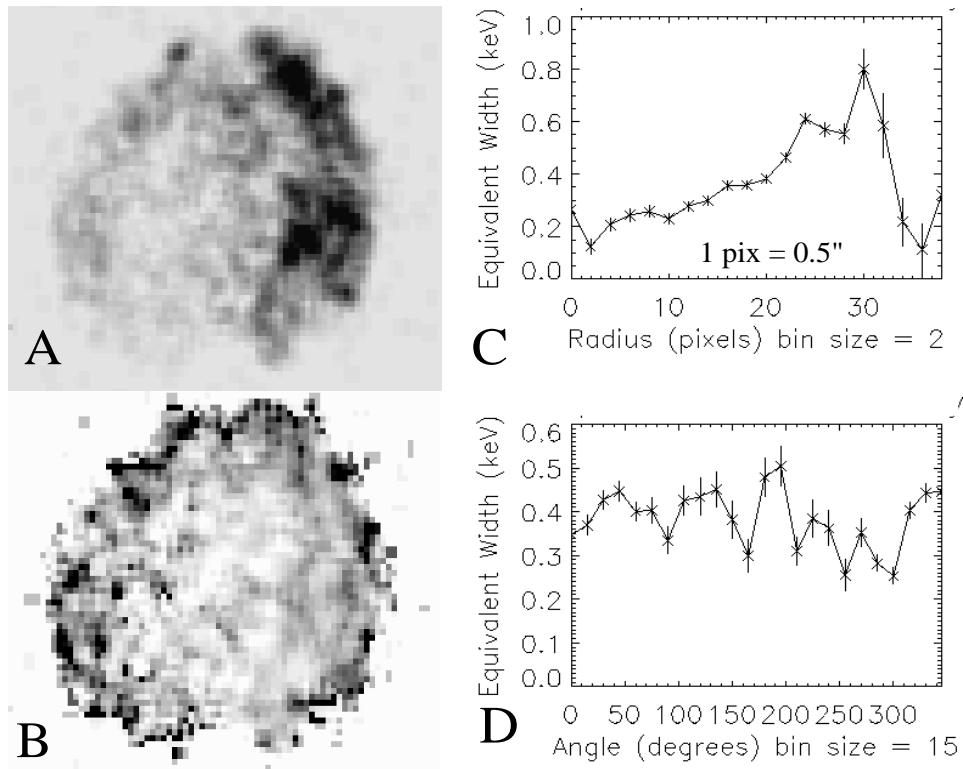


Figure 2. Narrow Band imaging in He-like Si. On the left, the continuum subtracted (A) and equivalent width (B) images. On the right, the radial (C) and azimuthal (D) dependence of the equivalent width.

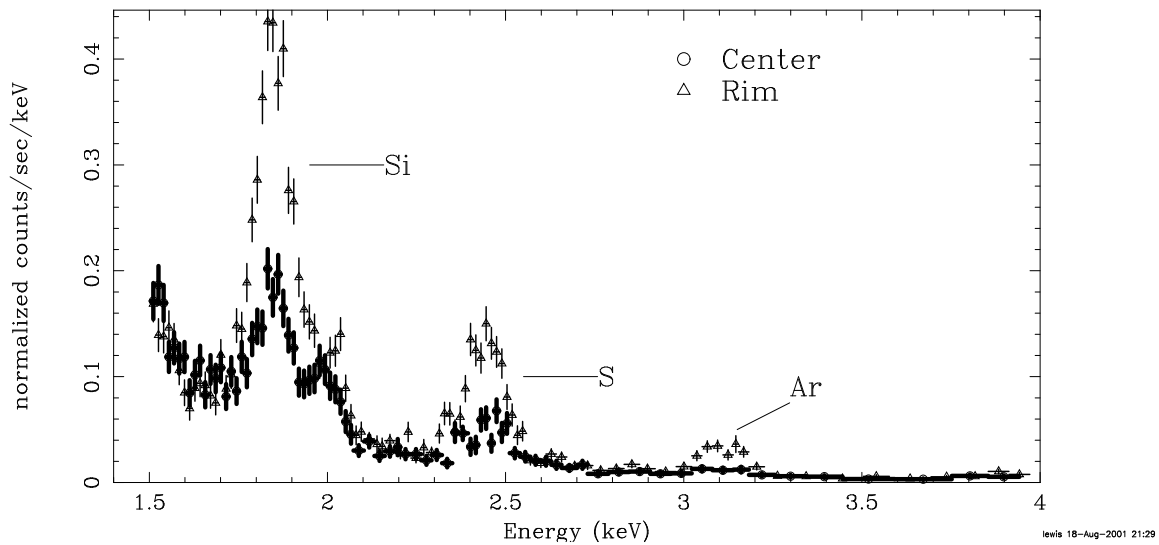


Figure 3. Comparison of the Si, S, and Ar line strengths in the inner and outermost rings.

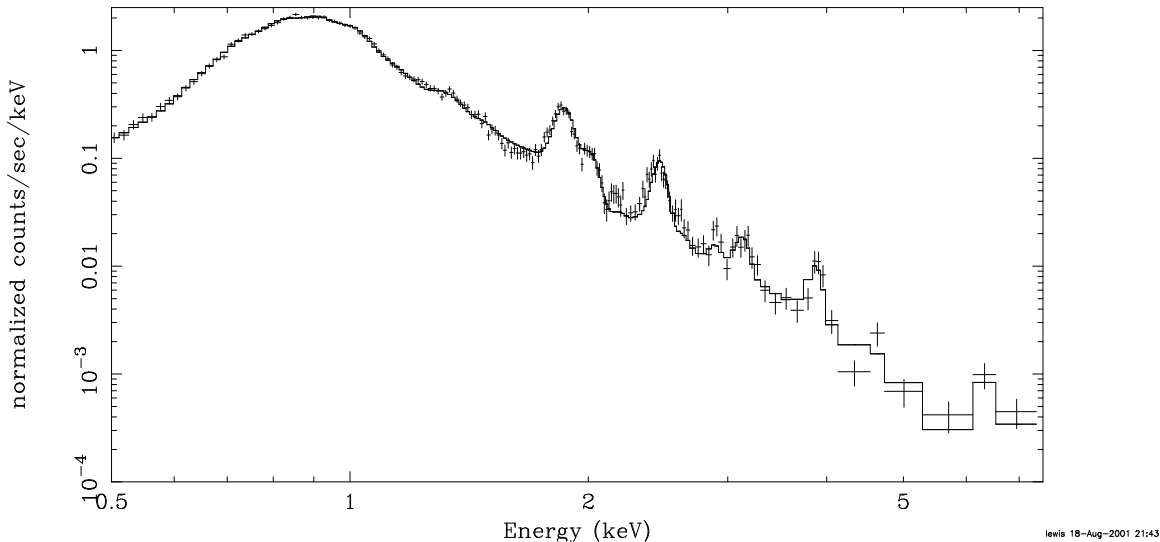


Figure 4. An example model fit for one of the rings. Note that the overall agreement between the data and model is excellent. However, there are a few lines, particularly from the  $K\beta$  ( $n=3$  to  $n=1$ ) transitions, which are under-produced, indicating that the electron temperature may be higher than suggested by the model.

temperatures and ionizations of the different phases do not vary significantly from ring to ring. The parameters which change most dramatically are the abundances of Si, S, and Ar (Fig. 5). The abundances of these elements are relatively flat in the interior, then rise sharply at a radius of  $10''$ , similar to what is seen in the equivalent width plots (Fig. 2cd). Thus the increase in the equivalent width of Si, S, and Ar is due to an increase in the abundance of these elements as opposed to a temperature or ionization variation. This radial stratification of the Si-burning products is most certainly a product of the supernova explosion itself.

#### 4. Conclusions

This high resolution *Chandra* observation has revealed brightness variations on the sub-arcsecond level. We believe that many of the variations are due to density inhomogeneities in the surrounding medium.

N103B appears to be very well mixed macroscopically and we see no evidence for bullets of ejecta, as seen in many galactic remnants such as Cas A (Hughes et al. 2000). This is partly due to the fact that the physical resolution element is  $\sim 10$  times larger in the LMC than within the galaxy. The plasma appears to possess three distinct thermodynamic phases; on a microscopic level, N103B is still quite clumpy. In particular we see evidence of a hot ( $\geq 3$ keV), low ionization ( $n_e t \sim 10^{10-11}$ s/cm<sup>3</sup>) Fe component in the plasma such as that seen Tycho's SNR.

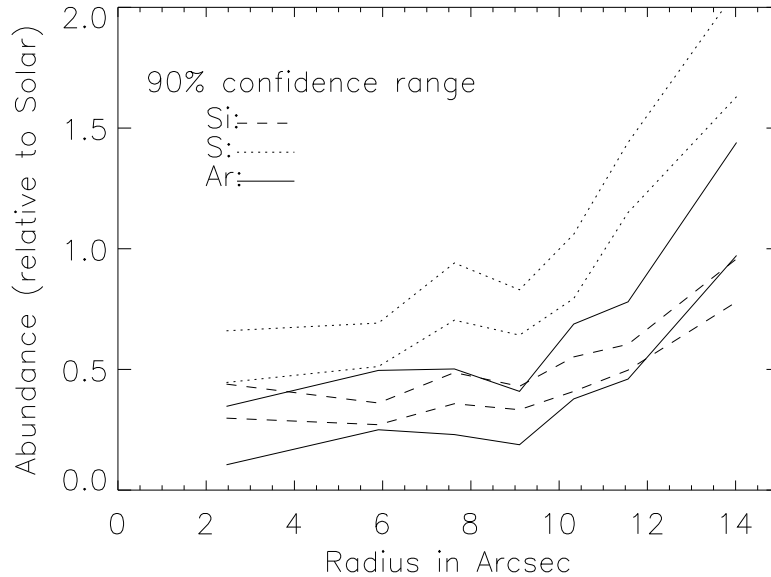


Figure 5. The 90 % confidence intervals for the abundances of Si, S, and Ar. The increase in the abundances far exceeds the random fluctuations, which are within the error bars.

We see an increase in the equivalent widths of Si, S, and Ar which are due to an increase in the abundances of these elements, as opposed to a change in the temperature or ionization state. This radial abundance stratification is most certainly a product of the explosion itself, as opposed to a variation in the surrounding medium. Future work will focus on the spectral analysis on the non-radial variations in N103B, which should yield interesting information on the interactions between this young supernova remnant and its unusual environment.

## References

- Dickel, J. R. & Milne, D. K. 1995, *AJ*, 109, 200  
 Hughes, J. P., Hayashi, I., & Koyama, K. 1998, *ApJ*, 505, 732  
 Hughes, J. P., Rakowski, C. E., Burrows, D. N., & Slane, P. O. 2000, *ApJ*, 528, L109  
 Hwang, U., Hughes, J. P., & Petre, R. 1998, *ApJ*, 497, 833  
 Russell, S. C. & Dopita, M. A. 1992, *ApJ*, 384, 508  
 Townsley, L. K., Broos, P. S., Chartaws, G., Moskalenko, E., Nousek, J. A., and G. G. Pavlov 2001, *NuclIM*, submitted  
 Townsley, L. K., Broos, Nousek, J. A., and G. P. Garmire 2001, *NuclIM*, submitted  
 Williams, R. M., Chu, Y., Dickel, J. R., Petre, R., Smith, R. C., & Tavaréz, M. 1999, *ApJS*, 123, 467